

INTERNATIONAL ATOMIC ENERGY AGENCY
UNITED NATIONS EDUCATIONAL, SCIENTIFIC AND CULTURAL ORGANIZATION



INTERNATIONAL CENTRE FOR THEORETICAL PHYSICS
34100 TRIESTE (ITALY) - P.O.B. 500 - MIRAMARE - STRADA COSTIERA 11 - TELEPHONE: 2240-1
CABLE: CENTRATOM - TELEX 660095-I

H4.SMR/167 - 14

SCHOOL ON PHYSIC IN INDUSTRY

27 January - 14 February 1986

" PHYSICS IN PETROLEUM INDUSTRY "

presented by

B. SILBERNAGEL
Corporate Research Science Laboratory
Exxon Research and Engineering Co.
Clinton Townships (route 22 East)
Annandale, NJ 08801
U.S.A.

These are preliminary lecture notes, intended for internal distribution to participants only.

Papers in The Petroleum Industry

There are five papers to the industry:

- + Exploration
- + Production
- + Transportation
- + Refining
- + End Use

B.C. BILBURN
in February 1986

LITERATURE PLAN

Introduction

- Scale of Energy Concerns
- Sources of Fossil Organics
- Exploration / Reserves

Papers on Exploration and Production

- Seismic Studies
- Other Papers: Gravity Surveying, Logging
- Microscopic Understanding / Facies Modeling

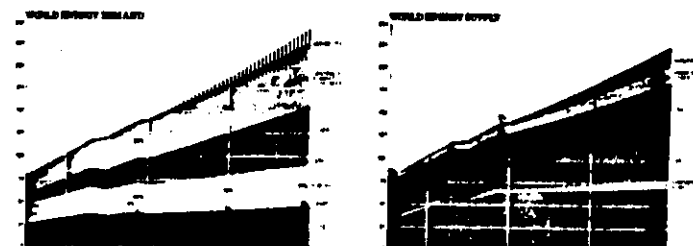
Papers on Oil Refining

- Residuum Hydroprocessing with Sulfide Catalysts
- Petroleum Refining with Noble Metal Catalysts
- Theories of Catalytic Activity

Problems Have Historically Been Very Complex

- + Exploration - Complicated geological structures
- Complex seismic data
- + Production - Heterogeneous reservoirs
- Borehole fluid modeling
- Organic-mineral interactions
- + Transportation
- + Refining - Complex, varied organic mixtures
- Little known about catalysis
- + End Use - Combustion under complex conditions
- + Great advances in Experimental Techniques, Theoretical Analyses Have Made These Problems More Tractable

Energy Is A Major, Increasing Concern



- Half chance of decline
- Lesser Declining from Peak Demand
- On a Geothermal Course
- Power Demand to Power...

(See: - How Many Years Before...)

Fossil Fuels Reserves

- $2 \text{ Quads} = 10^{15} \text{ Btu's}$
- $\approx 172 \text{ MMbbl} \text{ of Oil}$
- $\approx 0.47 \text{ Trillion cubic feet of Natural gas}$
- $\approx 20 \text{ Btcs of Coal}$
- $\approx 2500 \text{ Tons of Uranium Oxide}$

Oil & Gas Reservoir Accumulations in Geologically Recent (Our 4 Geological Time Scale)

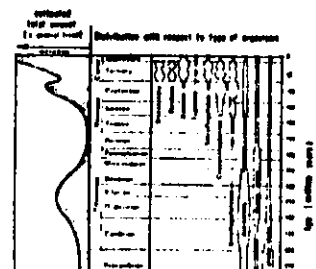
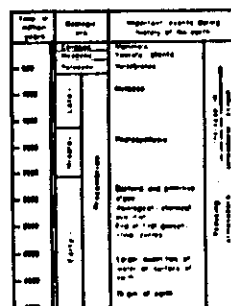


Fig. 1.1 Variations in percentages of land surface covered by ice during geological past. (Adapted from Tappin and Evansch, 1979) reprinted with permission and from publication of the Geological Society of America.

- Less than 0.1% of Oceans are Reservoirs

(Tappin & Ward, p. 1)

Major Shallow Areas and Shallow Seabed Hydrocarbon Concentration

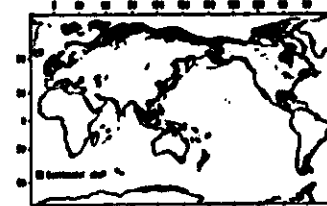


Fig. 1.2 Shallow areas of the world. Water depth is shallower than 200 m. Shallow areas belong to shelf areas.



Fig. 1.3 Present hydrocarbon production (Bsp. units in 10^6 m^3) in the world's oceans. Production is relatively high in coastal areas, especially in areas of major river discharge. The most active oil and gas areas are continental. (Adapted from Tappin and Evansch, 1979)

Table 1.1. Production of coastal regions in comparison to the open ocean. (Adapted after Sims, 1979)

Area	Area in km ² x 10 ⁶	Average production in 10^6 m^3	Total production in 10^6 m^3
Open ocean	75	50	3.75
Coastal areas	5	500	2.5
Areas with openings	0.4	300	0.12

(Tappin & Ward, p. 2)

Hydrocarbons Accumulate in Sediments

Sedimentary Basins



Types of Oil and Gas Accumulations



Although commonly depicted as discrete accumulations, oil and gas accumulations of large dimensions are often continuous along the reservoir rock, providing the oil and gas reservoirs with considerable amounts of oil and gas. Such accumulations, covering the entire reservoir, are referred to as giant fields. These are typical accumulations of major traps.

(Source: "New Data On Oil Gas" 1981)

Next Meeting with Brazil, Mexico, Canada

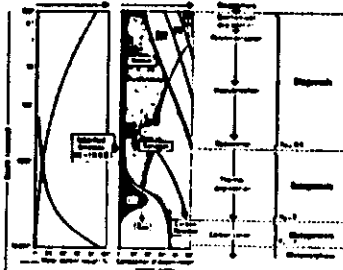


Fig. H-1-1. General scheme of evolution of the regressive model. From the health department undertaken in the environmental study of 10 countries during 40 years period 7.4 data and 14.6 items per each 2 years (1957-1997). Indication: 3, 5, 7, 9, 11, 13, 15, 17, 19, 21, 23, 25, 27, 29, 31, 33, 35, 37, 39, 41, 43, 45, 47, 49, 51, 53, 55, 57, 59, 61, 63, 65, 67, 69, 71, 73, 75, 77, 79, 81, 83, 85, 87, 89, 91, 93, 95, 97.

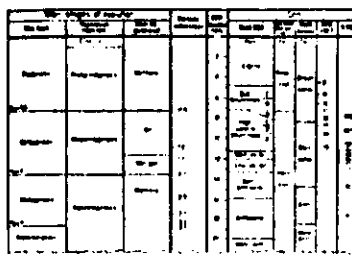
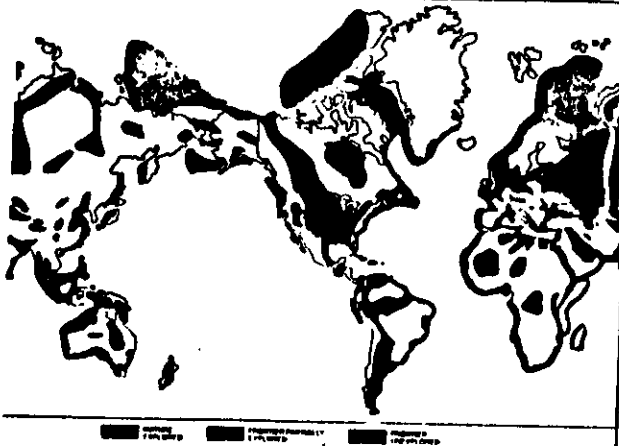


Fig. B1.2. Mean stages of maturation of the oocyte smear. The stages are divided into 3 groups after 1200×10^{-6} and the 1200 scale of Hwang et al. (1977) are given for comparison, and show the dependence on age and time. (A: Oocytes from women aged 20-24; B: women aged 30-34; C: oocytes from women aged 35-40). (Reproduced from Hwang et al. 1977, International Conference on Fertilization, 1975; Hwang et al. 1978; Sato et al. 1978).

Page 4 out of 10

Practical Geostatistics, Second



(From: "The Dark Sister," etc.)

Comm. Ch. 10000 New Executive Rd., St. Catharines, Ont.

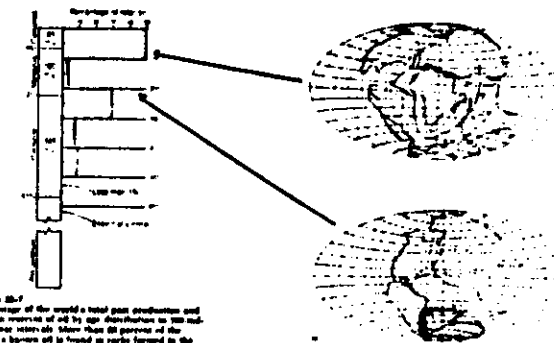


Figure 20-7
Percentage of the world's total past production and
present reserves of oil by age distribution as of 1970.
Less than 10 percent of the
world's known oil is found in rocks formed in the
last 100,000 years.

(*Gray & Gray, "P. M."*)

Forms of Drilling and Oil Traps



Figure 3 The Petroleum Sector Is the Americas' Oil-Heavy Sector: 40.5% of all the crude oil and 30.9% of all the natural gas consumed in the

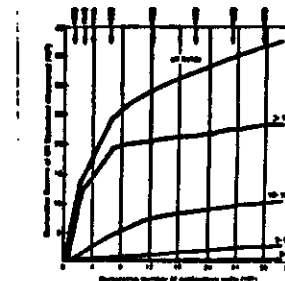


Figure 4. Within the system of parentheses indicated in the Panchromatic Plate, the area from which the samples were taken is delineated by a line in which the paleozoic rocks, and unconformities in these rocks are plotted against the total cumulative number of euryhaline cells. It shows that the higher layers contain the greatest numbers. The 4. Mark, which is the uppermost layer, contains 1.2 million cells; the 3. Mark, which is the middle layer, contains 1.1 million cells; the 2. Mark, which is the lowermost layer, contains 1.0 million cells; the 1. Mark, which is the lowest layer, contains 0.9 million cells; and the 0. Mark, which is the highest layer, contains 0.8 million cells. The figure also shows that the euryhaline history of the basin starts with the relatively stable sediments deposited prior to the 4. Mark, and ends with the highly unstable water prior to the 0. Mark, the highest stage of tidal and wavecutting, the major part of the tidal current disappeared.

(not on Dow, Bona fide in 1910)

Answers

Energy and Petroleum Survey

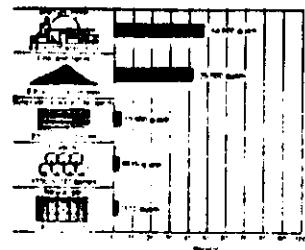


Figure 2-1
Estimate of recoverable world energy resources in 1970, measured in barrels (10¹²). Values converted to equivalent oil barrel equivalents through the factors given in parentheses. Values for coal and oil quality are based on recoverable resources for economic use in U.S. at 1970 prices. Natural gas reserves are 196,000 barrels or 8% percent of the total.

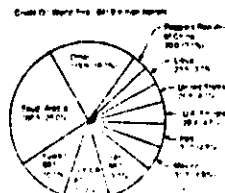


Figure 2-2
Estimate of world recoverable energy resources in 1970, measured in barrels (10¹²). Values converted to equivalent oil barrel equivalents through the factors given in parentheses. The 1970 values for oil and natural gas are based on recoverable resources for economic use in U.S. at 1970 prices. Natural gas reserves are based on data in Table 2-2 because natural gas liquids are not included in the oil pool for use in the United States. Other sources: EIA (Department of Energy).

(Russia & Soviet Union, "Soviet")

Observations from General Survey

- Large, But Firing Energy Reserves
- Petroleum & Relatively Small Fraction
 - For Fuels ~50% of our current energy needs
- Process of Fossil Hydrocarbon Preservation is Delicate
- Generation is Process very More Complex
- More Efficient Use of Non-Petroleum Resources



Fig. V-1
World distribution of petroleum reserves by group of countries owned by different countries. One of the criteria is retained in the location of most recoverable reserves. Adapted with changes from Bissell et al. (1972) estimates of the ownership of 170 oil & gas fields. (A) before 1950 and (B) since 1950.

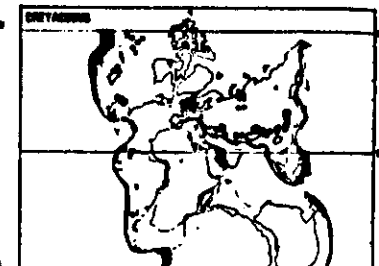
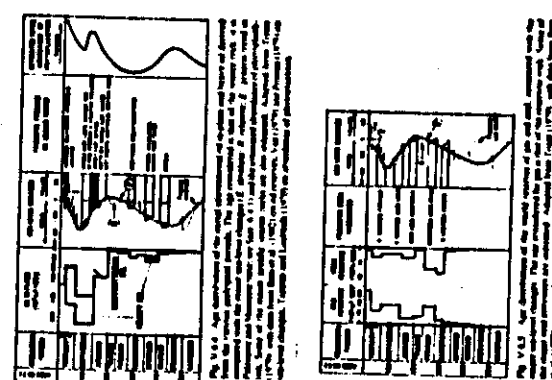


Fig. V-2
World distribution of petroleum reserves by group of countries owned by different countries. One of the criteria is retained in the location of most recoverable reserves. Adapted with changes from Bissell et al. (1972) estimates of the ownership of 170 oil & gas fields. (A) before 1950 and (B) since 1950.



Fig. V-3
Distribution of petroleum reserves by group of countries owned by different countries. One of the criteria is retained in the location of most recoverable reserves. Adapted with changes from Bissell et al. (1972) estimates of the ownership of 170 oil & gas fields. (A) before 1950 and (B) since 1950.



SOURCE OF OIL EXPLORATION

OIL SOURCE: Rock vs. Seal Caves

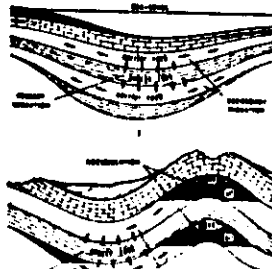


Fig. 10.11 Formation of oil and gas accumulations: a) diagenetic processes of primary and secondary migration in the early and advanced stage of lower evolution; b) final phase of primary and secondary migration; c) Advanced stage of primary and secondary migration and formation of accumulations.

(Tietz & Welte, Pg. 5)

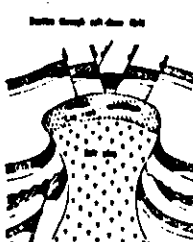


Fig. 10.12 Seals provide traps for oil/gas accumulations with oil phase distributed after 100 m.

Surveys for Seismic Prospecting Surveys

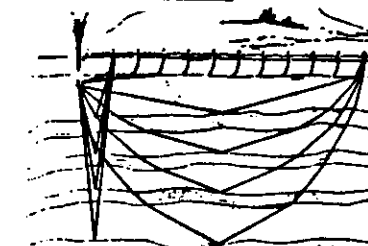


Fig. 10.13 Recovery of reflections from a subsurface geological horizon by seismic waves. From T. I. to the right the wavelet is reflected from the interface between the upper and lower layers. The reflection is measured on the seismogram and recorded by a seismograph. The time interval between the reflection and the direct wave is called the two-way reflection time in four times, and the distance between the reflection and the direct wave is called the reflection distance or round-trip time in four times.

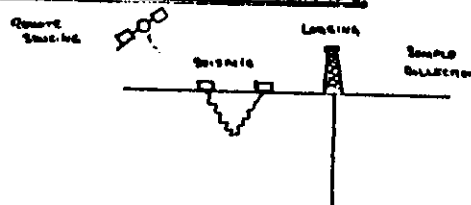
Fig. 10.14 A seismic reflection method. A strong downward impulse generates seismic waves which are reflected back from different layers and return. The reflections are measured on the seismogram and recorded by a seismograph. The time interval between the reflection and the direct wave is called the two-way reflection time in four times, and the distance between the reflection and the direct wave is called the reflection distance or round-trip time in four times.

Fig. 10.15 A seismic reflection method. A seismic reflection method. A seismic reflection method.

Fig. 10.16 A seismic reflection method. A seismic reflection method.

(Larin, Physics
Teacher, Pg. 19 (1976))

SEVERAL SOURCES OF GEOPHYSICAL INFORMATION



* Remote Sensing

- SPECTRAL REFLECTANCE
- SPECTRAL EMISSION
- THERMAL INFRARED
- RADAR

** Gravity and Magnetic Surveys

- GEOFONDS AND RADAR SURVEYS ZIL, 781 (1971)

- TIEZT & WELTE, 1981

*** Sample Extraction

- GEOMATERIAL & MINERALS ANALYSIS

SEISMIC ENERGY SOURCES

Fig. 10.17 A large underground explosion is a source of seismic waves. The energy of the explosion is converted into seismic waves. The energy of the explosion is converted into seismic waves.



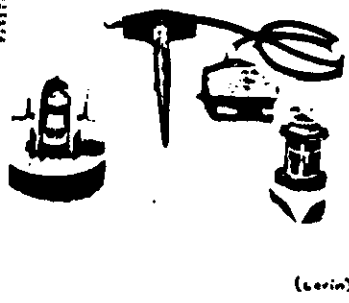
(Larin)



Fig. 10.18 A seismic source used to generate seismic waves. A series of seismic waves are generated by the source ship which pulls the detector cable.

Sonic Detectors (continued)

Fig. 3. Three methods used to record seismic waves and their interpretation by the author. Top: Seismograph, a device which records the time interval between the first and last reflections from different layers of rock. The top part can be rotated to measure the angle of reflection.



(Loring)

Data Collection and Analysis Strategy

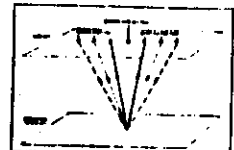
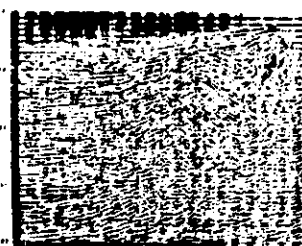


Fig. 4. Schematic of a method of collecting reflected energy of reflecting waves or an interface between two media. A source emits waves which travel through one medium and reflect off an interface of the other. A receiver picks up the reflected waves and measures the time interval between the source and the point of reflection to determine the distance to the interface in seconds. The time interval is converted to distance by the formula: $D = \frac{1}{2} C T$ where D is distance, C is velocity of wave propagation, and T is time interval in seconds.

(Loring)

Fig. 5. A typical series of seismic data often recorded by one source and receiver. The data are plotted on a grid system with depth on the vertical axis and time on the horizontal axis. The data are plotted in a series of vertical columns, each column representing a different time interval. The data are plotted in a series of vertical columns, each column representing a different time interval. The data are plotted in a series of vertical columns, each column representing a different time interval.



Well Logging - Physical Properties Down the Well

- + Electrical
- + Nuclear
- + Sonic

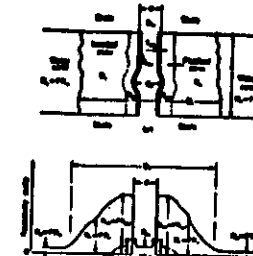
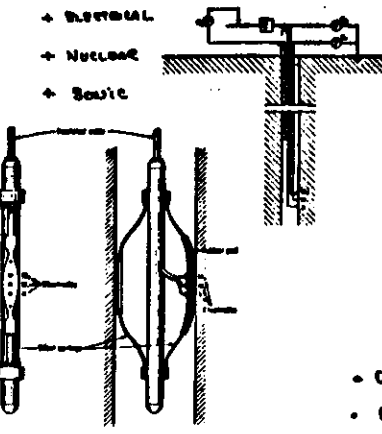


Fig. 6. (a) Well bore and probe descended down a well bore; (b) resistivity graph. After G. J. Price, Oil Field Handbook, Vol. 1, Geophysical Log, 1960, Texaco Oil Co., Inc., 1960.

- Complex Environment
- Correlation-Based
- Existing (Geologic Structure) (See Previous "Evaluation of Well Logs" section, 1961)

Electrical Log, Resistivity Properties



Fig. 7. (a) Resistivity log, showing the resistivity of the rock, a lithological sample, and the resistivity of the water in the rock. (b) Resistivity log, showing the resistivity of the rock, a lithological sample, and the resistivity of the water in the rock. (c) Resistivity log, showing the resistivity of the rock, a lithological sample, and the resistivity of the water in the rock.



Fig. 7. (b) Resistivity log, showing the resistivity of the rock, a lithological sample, and the resistivity of the water in the rock. (c) Resistivity log, showing the resistivity of the rock, a lithological sample, and the resistivity of the water in the rock.

(See Loring, Geology of Petroleum, German, 1967)

Sonic Log / Neutron Log Seismic Wavelet

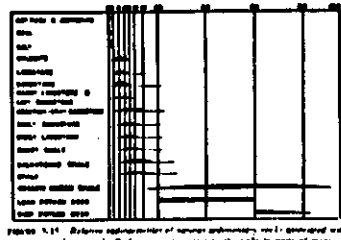


FIGURE 1.1: Schematic representation of seismic wavelet. (Left) Schematic representation of seismic wavelet. (Right) Amplitude response in units of neutron count per second per gram of rock. (Courtesy from Russell, Bull, and Baker, *Seismic Pulse*, Vol. 23 (1962), p. 1772)

HORIZONTAL CONDUCTIVITY

CONDUCTORS: U, Th, K

T = 2-2 MeV

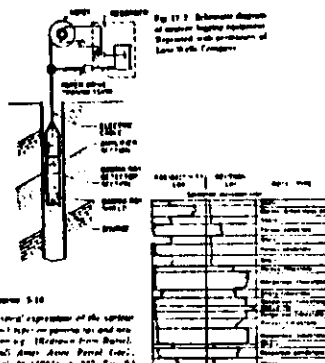


FIGURE 1.2: Schematic representation of the seismic wavelet. (Left) Schematic representation of seismic wavelet. (Right) Amplitude response in units of neutron count per second per gram of rock. (Courtesy from Russell, Bull, and Baker, *Seismic Pulse*, Vol. 23 (1962), p. 177, Fig. 2)

(Ref. University)

Sonic Log / Neutron Log Processing, Material Properties

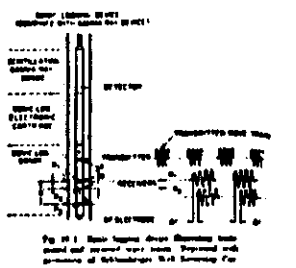
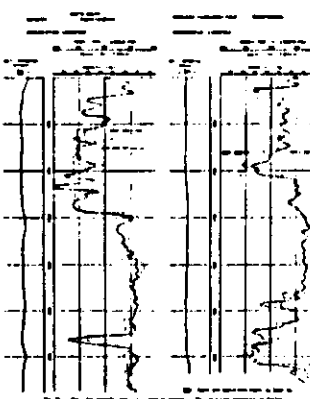


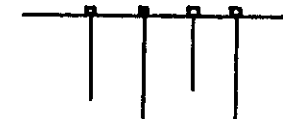
FIGURE 1.3: Schematic representation of seismic wavelet. (Left) Schematic representation of seismic wavelet. (Right) Amplitude response in units of neutron count per second per gram of rock. (Courtesy from Russell, Bull, and Baker, *Seismic Pulse*, Vol. 23 (1962), p. 1772)



(Ref. Pielou, "Ecological Methods", 1961)

Production of Discovered oil is a challenge

- OPTIMUM RATE OF WITHDRAWAL
- OPTIMUM PLACEMENT OF WELLS
- DRAINAGE, THICKNESS METHODS
- MAINTAINING OIL FLOW
- CAPILLARY FORCES
- OIL-MINERAL INTERACTIONS



⇒ GOAL: A microscopic understanding of fluid flow in rocks.

Powerful You Have for Assimilate Porous Media Properties, Interaction: Particles

- COMPLEX DIMENSIONALITY: - Space is 3 PLANE, COMPLEX POROUS MEDIA: $N(R) = N(2R) \approx R^D$

$$\text{Volume } 2 = \frac{1}{2}R, \quad N(R) = N(2) R^D$$

D = Number Dimension

For the boundary of porous medium $R + R_0 + \Delta R \approx g(R) \Delta R$

$$R^{D-1} g(R) \approx R^{D-1}$$

$$\therefore g(R) \approx \frac{\text{const.}}{R^{D-1}}$$

Self-Similarity - A part of the system contains all information of the whole.

→ Limited Range of Application

Sedimentary Structures Can Be Described By Fractals

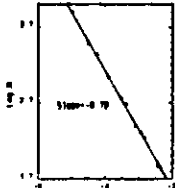


FIG. 1. A log-log plot of the number of geometric elements of size E per unit length vs. the size E for various rock facies (modified from Cormier, 1986).



FIG. 2. A log-log plot of the power-law density parameter, α , for a quartzarenous sandstone from the Tigray. The slope of the straight line was taken from core and outcrop data collected on a fracture surface. The scatterplots were taken from 32-bit images of polished rock thin sections. The units of measurement are arbitrary.

TABLE 1 Results of SEM measurements on various sandstones

Sample	Parent Dimension	L (nm)	Calculated	Measured
Tight gas sand core	3.51	25	67	53-58
Tight gas sand core	3.60	6	70	68-70
Cormier	2.70	50	10	11-12 ^a
Meng	2.81	50	14	16.0
S. Pierre	1.77	50	31	38-39

(Keller and Thompson, Rep. Berlin 9, 1985)

The Fractal Growth of Vuggy Fingers

- Provides Unique Method to Study Vuggy Porosity
- PARTICULARLY IMPORTANT FOR Secondary AND TERTIARY OIL Recovery



FIG. 3. Fracture network developed in a core of strong fine-grained sandstone. The fractures are irregular and have been partially replaced by vuggy porosity. The pore spaces between vugs are interconnected. The pore spaces are larger than 1 mm in diameter. The water-saturated rock has a porosity of 15% and a permeability of 100 mD. The vugs have an average porosity between 0.5 and 0.7 depending on the size of the vugs.

(Hermans, Deneau, and Shantz, Nature 306, 401 (1983))



FIG. 4. A photograph of a fractured rock sample showing vuggy fingers.



FIG. 5. Inverse proportionality of the dimension of D versus the size of the largest finger L . The slope of the straight line given is D , from which we find $d = 1.9$.

Conclusions:

- Exploration and Production Are Formidable:
 - Heterogeneous Structures
 - Complex, Multiphase Interactions
 - Need for High Spatial Resolution
- Current Computational, Experimental, Theoretical Developments Hold Great Promise for Quantitative Advances
 - Supercomputers
 - High Sensitivity Microscopy
 - New Theoretical Approaches: Fractals

Purposes of Petroleum Refining

General Objectives:

- Component Separation
- Mineral / Metals Removal
- Heteroatoms (Nitrogen, Sulfur) Removal
- Molecular Weight Reduction
- Blending / Product Formulation

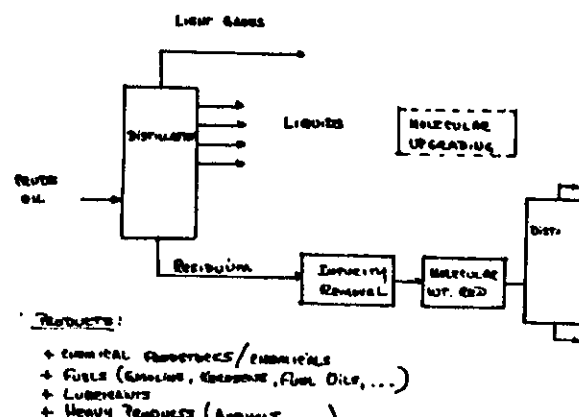
=> Done by a combination of Purposes (separations)
and Chemistry (conversion)

Chemical Conversions are Accomplished by Several Means

- Thermal Treatments
- Catalysis (Heterogeneous or Homogeneous)
 - Minerals (Clays, Zeolites, ...)
 - Metals (Transition Metals, Noble Metals, Alloys)
 - Others (Sulfides, Oxides)

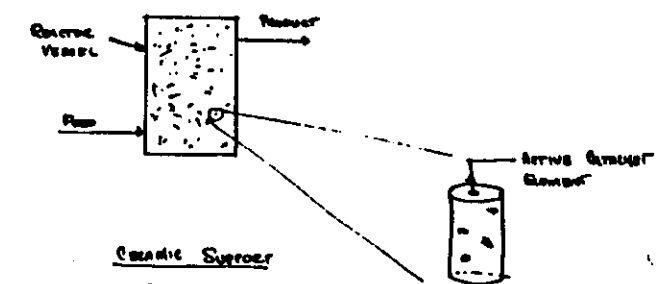
(Dr. G.M. Satterfield, Heterogeneous Catalysis in Petrol., McGraw-Hill, 1980)

General Refining Strategy



(The Petroleum Hand Book, Elsevier, 1988)

Heterogeneous Catalysis: A Schematic



Catalytic Suspender

- Pore Volume
- Pore Size Distribution
- Nanoscale Dimensions
- Mechanical Properties

Hydrodeactivation Catalysis: A Specific Example

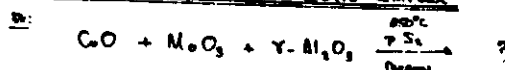
GOAL: TO UPGRADE CRUDE OILS AND RESIDUA (300-550°)

KUWAIT	JORDAN Heavy	MARIBAN Heavy
SULFUR (wt.%)	4.21	2.78
MERCURY (ppm)	58	145
NIQUEL (ppm)	12.7	88.6
C ₄ AROMATICS (wt%)	3.7	8.6
CHART. CARBON (wt.%)	9.8	10.0
		10.1

- GOALS:
- DEWATERIZATION
 - HETEROCYCLIC REMOVAL (S + N)
 - MOLECULAR WEIGHT REDUCTION

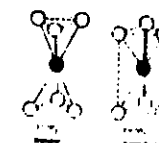
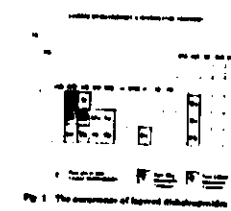
(See, Chapter Deactivation 6 (Boudelle, 1980), p.552)

The Operating Catalyst is Quite Complex



- Heterogeneous Oxides / Sulfides
- Great "Promoter" (relationship To Mo?)
- Alumina Surface Effects
- Deposited Carbon
- Deposited Metals (V, Ni, ...)
- ⇒ Can One Derive Analysis?
- + Heterogeneous Mechanisms?
- + Active Sites?

NiS is one of a Large Class of Layered Sulfides

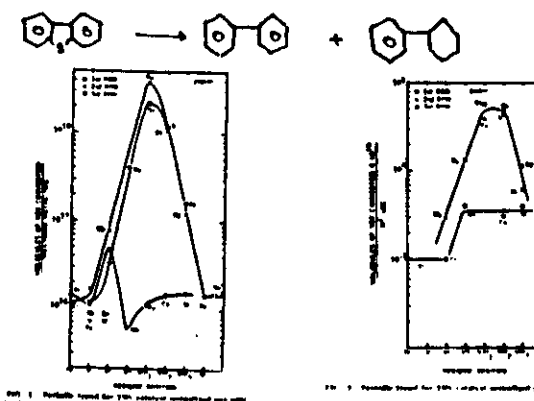


- + SUPERCONDUCTORS, SEMICONDUCTORS, METALS
- + NON-STOICHIOMETRY
- + INTERCALATION

(See, Boudelle, Rev. Sci. Res. 21, 221 (1982))

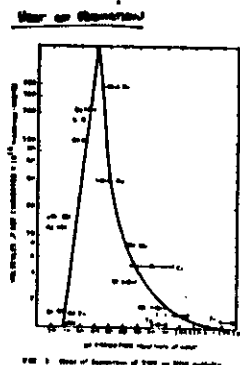
Model Reactions Phase Catalysts

EXAMPLE: DISUBSTITUTED THIOPHENES DESULFURIZATION



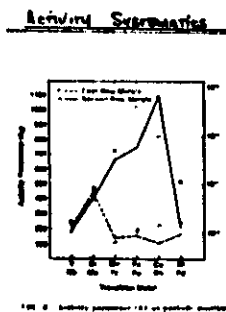
Source: Boudelle, Comptes Rendus, Paris 291, 301 (1980))

Relation To Some Physical Properties



The graph plots $\frac{1}{\tau}$ (sec $^{-1}$) on the y-axis against $\frac{1}{\alpha}$ (cm $^{-1}$) on the x-axis. The y-axis has major ticks at 0.00, 0.01, 0.02, 0.03, and 0.04. The x-axis has major ticks at 0.00, 0.01, 0.02, 0.03, 0.04, 0.05, 0.06, 0.07, 0.08, 0.09, 0.10, and 0.11. A series of data points are plotted as open circles, and a straight line of best fit passes through the origin, indicating a linear relationship.

(१२०५)



The diagram illustrates the memory hierarchy with four levels:

- Level 1:** Registers (labeled R_{1_1}, R_{1_2}, \dots)
- Level 2:** Cache (labeled C_{2_1}, C_{2_2}, \dots)
- Level 3:** Main Memory (labeled M_{3_1}, M_{3_2}, \dots)
- Level 4:** Disk (labeled D_{4_1}, D_{4_2}, \dots)

Arrows indicate the flow of data from Level 1 to Level 4, with a feedback loop from Level 4 back to Level 1.

(Continued)

Oxygen Consumption, Surface Area of R.E., Track WDS Activity

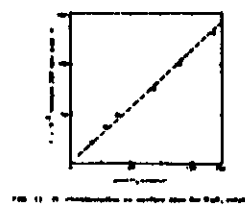


Fig. 1. A comparison of water flow and wave

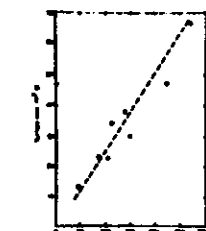
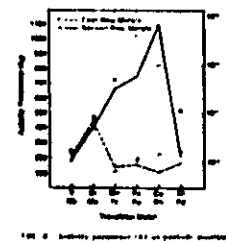


圖 11. 電子商務與傳統零售業之競爭

- External Review
 - P.S. Has a Specific Responsibility - Not Laymen

Page 1

Activity Spectra and Electronic Band Responses



The diagram illustrates the hierarchical organization of memory structures:

- Level 1:** Registers (R1, R2, R3, R4) are shown as small boxes.
- Level 2:** A stack of four boxes labeled "Memory".
- Level 3:** A stack of four boxes labeled "Buffer 1".
- Level 4:** A stack of four boxes labeled "Buffer 2".

A vertical line on the left indicates the boundary between Level 1 and Level 2. The bottom row of boxes is enclosed in a bracket labeled "Memory" above it, and the top row of boxes is enclosed in a bracket labeled "Buffer 1" above it. The bottom row of boxes is also enclosed in a bracket labeled "Buffer 2" above it.

(Continued)

Magnetic Susceptibility, O₂ Consumption and ESR for NiS.

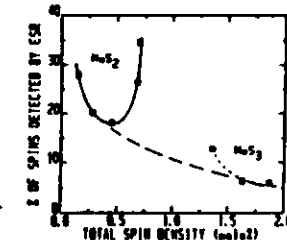
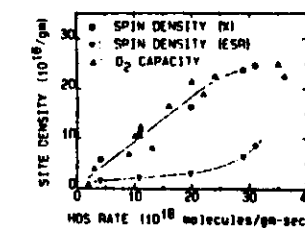


Fig. 2. Representative curves of the absorption coefficient μ versus wavelength λ for the following samples:
1. Sample 1000-1000000 - mean mass 1000 g./mole. Per
chlorate, 100% Crystalline, $\mu = 1.1 \times 10^4$ cm.⁻¹. Per
chlorate, 100% Crystalline, $\mu = 1.0 \times 10^4$ cm.⁻¹.
2. Sample 1000-1000000 - mean mass 1000 g./mole. Per
chlorate, 100% Crystalline, $\mu = 1.1 \times 10^4$ cm.⁻¹.
3. Sample 1000-1000000 - mean mass 1000 g./mole. Per
chlorate, 100% Crystalline, $\mu = 1.1 \times 10^4$ cm.⁻¹.
*(S. L. Johnson, Jr., Jr., ACS Div. Div.
50, 204 (1948))*

Sources Area Does Not Track NBS Activating Fig. MoS₂

NBS activating Does track

- O₂ concentration AND
- Mo⁶⁺ Dimer Dissolving from
Electron Beam Irradiation

Sources Area Sites Are Active

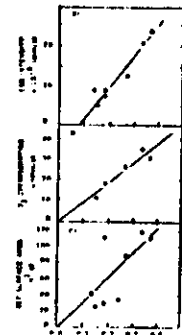
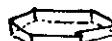


Fig. 1. Product particles at 2000 particle per liter, dose 1000 Rads to activate. (1000 eV electron, 1000 rad/min, 1000 volt/cm)

(Suzuki, Pichot, Renuart, J. Electron
(1))

Electron Microscopy on Mo₂ Oxide



Fig. 2. Unoxidized Mo₂. On oxidized
particle of Mo₂. Dimension of crystal shown in Fig.
1. (a) unoxidized Mo₂ (b)
Mo₂ oxidized Mo₂ (c)

- Transistor Function Not Consistent in Three Oxide-Sulfide Systems

(Takemoto, et al., J. (p. 22, 514))

Area Spacings and Structure Data Location of the Cobalt Reduction Areas

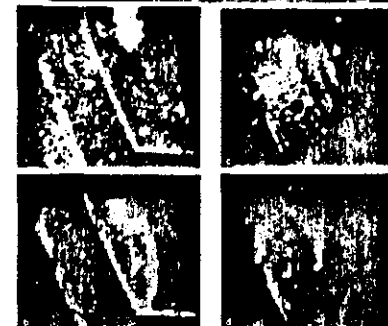


Fig. 3. Auger elemental signal mapping showing presence of Co and O on the surface of oxygenated cobalt oxide in a cobalt reduction area (1000 rad).

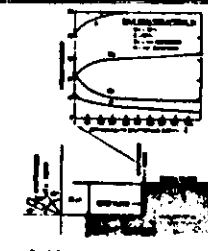


Fig. 4. Schematic diagram of specimen holder
by means of which powder

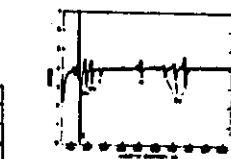


Fig. 5. Auger spectrum from the edge of the oxygen
layer containing 10% of the cobalt surface. (Co + O
and Co₃O₄) (1000 rad of oxygen dose)

(Takemoto, et al., J. (p. 22, 514))

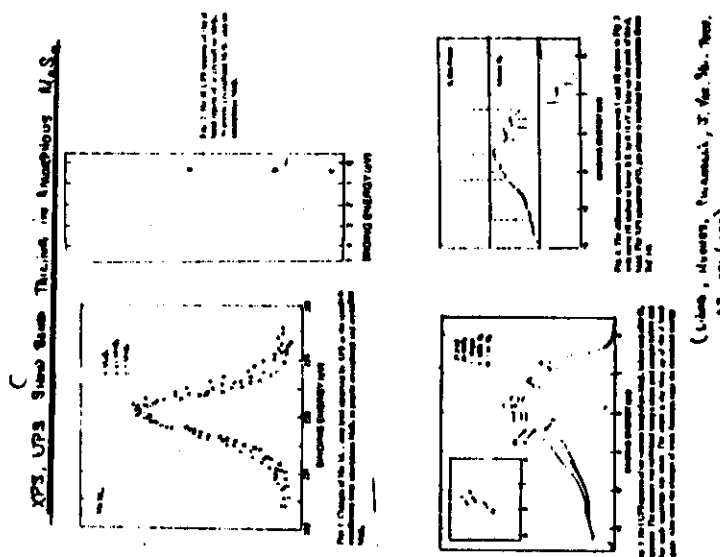


Fig. 6. SEM image showing the
surface of the Mo₂ oxide.

(Takemoto, et al., J. (p. 22, 514))

Nineteen Specimen Discusses Color Series on Catalogues

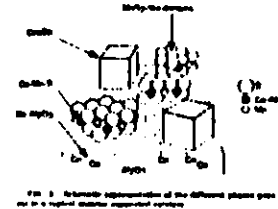


Fig. 3. Schematic representation of the different phase regions in a typical carbon-supported catalyst.

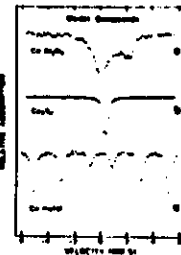


FIG. 1. Examples of different types of clusters of nuclei on grounds. See Fig. 2(a), (b), (c), (d), (e) (f) (g) (h) (i) (j) (k) (l) (m) (n) (o) (p) (q) (r) (s) (t) (u) (v) (w) (x) (y) (z).

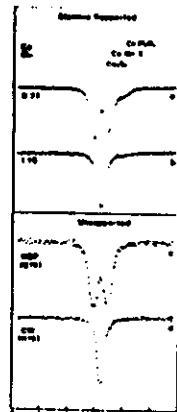


FIG. 3. Examples of type spectra of standard supported and unsupported C-13 materials. The unsupported materials were prepared using the homogeneous α - β -radiation method (HCP), mixed and the protonation of the carbon-supported materials (figure on right) was done at 40°C .

{Tengde & Clausen, Far. Rev. Sci. Ind. 36, 395 (1901)}

Catalytic Activity Trends Against C₆-H₅-S Phas.

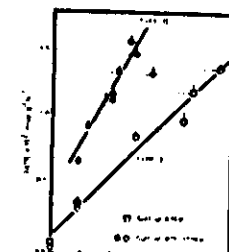


FIG. 3. Apparatus showing the principle of the Δ - Δ method for the determination of relative densities of different temperatures.

(Торгов аудио газета)

Investigation into Surface Properties of $\text{S}/\text{K}_2/\text{H}_2\text{O}_2$ Catalysts

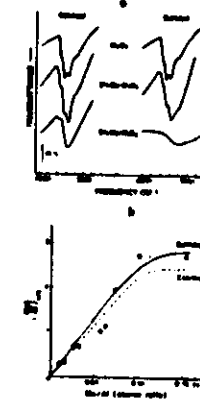


FIG. 9. Far infrared spectra of surface coatings of groups of aluminum and thorium hydroxides by the reduced and unreacted epichlorohydrin- H_2O (1:1) mixtures of the $\text{M}-\text{OH}$ hydroxides.



FIG. 6 Effect of Cu loading on absorption and activity of a series of sulfated Cu-Mg-Al₂O₃ catalysts. (a) UV spectrum of Cu adsorbed on the Cu-0.1% to Cu-0.6% (b) Cu and the total framework (c) Total absorption (d) 0.05 M, aqueous (e) The phosphate (f) total parameter. (g) Data adapted from Ref. 26 and 27.

(Twelve to Twenty)

Catalytic Activity Trends Among C₆-H₅-B Phases

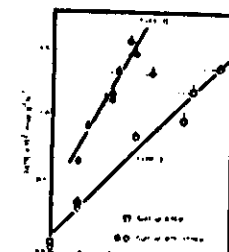
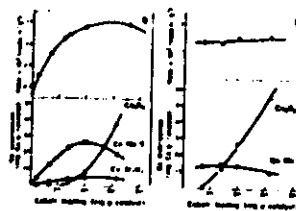


FIG. 3. Apparatus showing the principle of the Δ - Δ method for the determination of relative densities of different temperatures.

(Торгов аудио газета)

TRANS MANAGEMENT GROUP SMALL NO. 3, PETROLEUM AND CHEMICALS

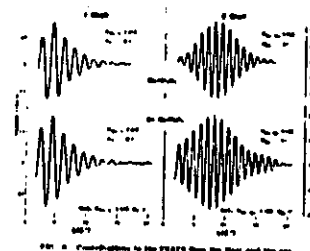


FIG. 2. Cross-sections to the 25470-Å line for He II and He III at 10¹⁰ cm⁻³, $T_e = 10^4$ K, and $\tau = 10^{-10}$ sec. The experimental data are shown with a full line whereas the theoretical curves are shown with a broken line. The quoted error

- ~ 10⁸
 - Evolution of Gneiss Features The No. Bears
 - Can appear to be one crystallite

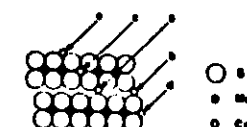


FIG. 8. Electrophoresis patterns of blood, with different proportions of a derivative, 50% fresh water extract, 50% "lysophosphatidylserine," 10% dried extract, 10% ether extract, 40% liquid plasma derivative, 10% aqueous extract, and 20%.

Dynamic Chemistry and Characterization in the study

To Understanding Catalysis

- Molecular Conversion Process
 - Products
 - Kinetics
 - Catalyst Chemistry Variations
 - Battery of Characterization Techniques
 - ESR
 - NMR
 - EXAFS
 - UPS, XPS
 - NMR
 - Microscopy, Microprobe
 - Magnetic Susceptibility
- In situ
- Molecular Absorption ...
 - Theoretical Self Consistency

